The Generation and Tracking of Mesh Objects in Image Sequences

Jui-Tai Ko, Bih-Wei Shyr, and Sheng-Jyh Wang
Department of Electronics Engineering, Institute of Electronics,
National Chiao Tung University, Hsin-Chu, Taiwan, R.O.C
Email address: shengjyh@cc.nctu.edu.tw
Tel: +886-3-5731878 Fax: +886-3-5724361

ABSTRACT

In this paper, we propose a new scheme that could automatically generate a hierarchical mesh structure for a real image and then use a nodal block matching to track this mesh structure in an image sequence. First, a three-layer pyramid is built by using a multi-resolution approach. For each layer, after extracting the high-curvature features, a linking procedure and a splitting process are applied to generate a compact set of representative points. By adopting the constrained Delaunay triangulation algorithm, the selected points can be triangulated into meshes. Starting from the coarsest layer to the finest layer, we further eliminate the duplicate nodes and then form a hierarchical mesh structure. Based on the hierarchical mesh structure and the intensity value at the mesh nodes and, we can progressively reconstruct an image with simple linear interpolation. Moreover, the motion of a mesh is tracked using a coarse-to-fine approach to lower the computational complexity.

Keywords: Mesh object, Image representation, Delaunay triangulation, Mesh object tracking

1. INTRODUCTION

In computer graphics [5], a mesh representation has been used as a model and conveyed to various applications. How to efficiently build a mesh model is one of the key technologies for these applications. In [7], an algorithm for generating a quadrilateral mesh from range data is proposed. Placing mesh nodes at beginning, the authors adjust the position of mesh nodes accordingly so that there are more nodes in curved regions and fewer nodes over smooth regions. Another mesh construction approach, which gradually deforms a primitive model to fit observed range data, can be found in [11]. However, the amount of data for these mesh-based applications are usually very large, especially when more details about the objects are required. To cope with this problem, a hierarchical model is employed and the model can be displayed optionally according to various requirements. A hierarchical mesh that adopts a node decimation procedure can be found in [6]. An approach that repeatedly subdivides a coarser model into a finer one has also been proposed in [8]. By using a mesh representation as an object descriptor, different objects may have different mesh structures. Based on this concept, object recognition can be done [9,10]. Even though there are so many applications that mesh can convey to, many researchers still try to extend the usage of mesh. In the context of MPEG-4, a mesh is an alternative representation of an arbitrary shaped object and it may further be applied to object-based video coding. In [14], Y. Wang et al. evaluated a mesh-based motion estimation in an H.263-like coder. Among the object-based applications, "mesh" has attracted the attention of many researches and many methods have been proposed for the generating and tracking of meshes in video sequences. Once a mesh representation can be generated, it can be used for multimedia editing and video object manipulation—e.g., replace objects in a scene, known as transfiguration [13]. Despite these applications relevant to MPEG-4, mesh is also used in image analysis, like pattern analysis, depth estimation in stereo imaging, etc. To build mesh for real images, Y. Wang et al. proposed a snake-based method [1,2]. According to an energy function that is depending on reconstruction error, image gradients, and mesh connectivity constraints, they deform a regular mesh to generate a scene-adaptive mesh. Based on a coarse-to-fine strategy, a hierarchical mesh is also generated. On the other hand, Tekalp et al. [15,16] developed a scheme to generate a hierarchical mesh that can be used for video coding. By removing a special set of mesh nodes, namely *an independent set*, a finer mesh can be divided into two layers: a coarser mesh and the refinement data. Thus, a hierarchical mesh can be built with a fine-to-coarse manner by repeating this node decimation procedure. Moreover, the discussions of avoiding patch overlapping and occlusion are also included.

2. BASIC CONCEPT

Our main concern is about how to generate a mesh to represent a real image. The desired mesh structure, same as others, requires that the image surface within each patch can be approximated by a plane. "Edge" is one kind of commonly used image features. It indicates the place where the intensity is very different on its two sides. We may allocate mesh nodes on

In *Image and Video Communications and Processing 2000*, Bhaskaran Vasudev, T. Russell Hsing, Andrew G. Tescher, Robert L. Stevenson, Editors, Proceedings of SPIE Vol. 3974 (2000) • 0277-786X/00/$15.00

the locations where the edge features occur to form such a structure. However, this kind of mesh structure would introduce a complicated reconstruction problem when trying to recover the original image. There is a 1-D example in Fig. 1 to illustrate this problem. Fig. 1(a) is a given intensity profile. With the edge points shown in Fig. 1(b), it's fairly difficult to recover the original profile because we don't know how or where the intensity value transits from one level to another around the edge feature. In this paper, we adopt a different type of feature — high-curvature features. A high-curvature feature indicates a place where the curvature of the image surface changes dramatically. In fact, a step edge would have two high curvature features so that the position of the edge (between these two high curvature features) and the intensity information can be recorded at the same time. With the high-curvature points in Fig. 1(c), we can do an easy reconstruction simply by using linear interpolation.

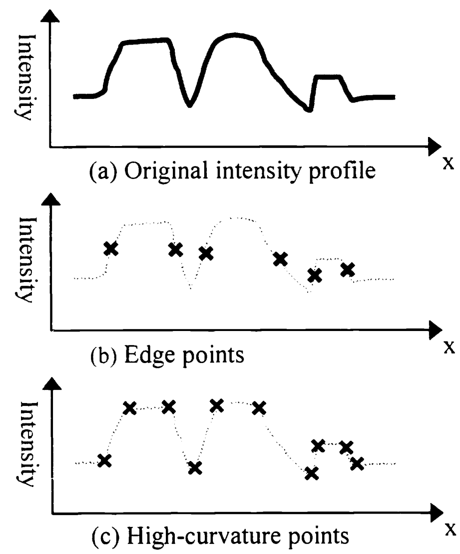

Fig. 1: Different types of features.

3. GENERATION OF STATIC MESH

The flowchart in Fig. 2 shows three basic procedures in our scheme. First, we extract high-curvature features for a given image. Generally, the number of detected feature points may be reduced to generate a more compact set of points. They can be further linked into curves if some of them belong to the same boundary. Each linked curve is then approximated by piecewise line segments. The two endpoints of these approximating segments would serve as the mesh nodes. With them, we can thus generate a mesh object by using the constrained Delaunay triangulation algorithm.

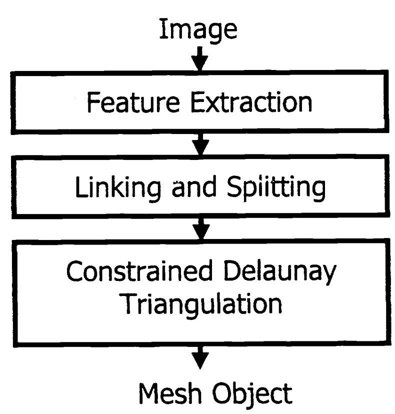

Fig. 2: The flowchart of mesh generation

3.1 EXTRACTION OF HIGH CURVATURE FEATURES

In this paper, we adopt the Jong-Wang operator [3] to extract the high-curvature features. This algorithm can accurately estimates both curvature magnitude and feature orientation. Based on some differential geometry analysis, the authors stated that the principal curvatures of an image surface around the point (x, y) may be estimated by calculating the eigenvalues of the matrix

$$M = \begin{bmatrix} \dfrac{\partial^2 f(x,y)}{\partial x^2} & \dfrac{\partial^2 f(x,y)}{\partial x \partial y} \\ \dfrac{\partial^2 f(x,y)}{\partial x \partial y} & \dfrac{\partial^2 f(x,y)}{\partial y^2} \end{bmatrix},$$

where $f(x,y)$ denotes the image intensity. Given M, two eigenvalues and two corresponding eigenvectors are calculated at each location (x,y). $\lambda_1(x, y)$ is the eigenvalue with larger magnitude. It indicates the maximum bending degree of the image surface around the pixel (x,y). On the other hand, $\lambda_2(x, y)$ is the eigenvalue with lower magnitude. Its corresponding eigenvector $\Lambda_2(x, y)$ would offer us the information about feature orientation. Fig. 3 shows an example and illustrates the extracted high-curvature features.

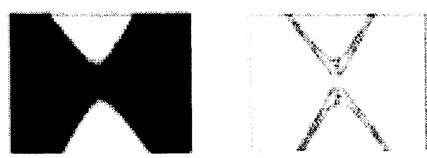
(a) (b)

Fig. 3: (a) A synthetic image (b) Detected feature points

3.2 LINKING OF FEATURE POINTS

3.2.1 SIMILARITY MEASUREMENT

To link a curve, we apply similarity tests to decide whether two adjacent feature points belong to the same curve. The tests take into account curvature strength, feature orientation, and some other constrains at the same time. Distinct test generates its relative similarity score and the degree of similarity can be measured as follows:

1) If the curvature signs of two neighboring features are opposite to each other, they can't be linked together and S_1 is set to zero; otherwise, S_1 is set to one.

$$S_1 = \begin{cases} 1 & \text{same sign} \\ 0 & \text{otherwise} \end{cases}$$

2) The two neighboring feature points must have similar orientations. The test on the orientation of features is measured by S_2 as:

$$S_2 = \begin{cases} \dfrac{TD_1 - DD}{TD_1 \cdot A_1} & \text{if } TD_1 > DD \\ 0 & \text{otherwise} \end{cases},$$

where TD_1 is the threshold of the direction difference; DD is the direction difference; and A_1 is an adjustable scalar. If the direction difference of these two points is smaller than the predefined threshold, we get a nonzero score. If the direction difference is too large, S_2 is set to zero.

3) As shown in Fig. 4, we check the angle $\angle$**DC**, which is the orientation of $\Lambda_2(x_0, y_0)$ and the orientation of $\overrightarrow{DP}$, which links ***P*** and **Q**. We set a limit on the angles between $\angle$**DC** and $\angle$**DP** and S_3 is defined:

$$S_3 = \frac{TD_2 - |\angle DC - \angle DP|}{TD \cdot A_2},$$

where TD_2 is the threshold of the angle difference and A_2 is an adjustable scalar.

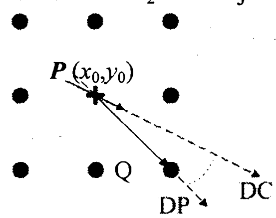

Fig. 4: Illustration of the constraint on the curvature direction and the linking direction

4) We apply a geometry constraint to prevent the linked curve from banding too much. The angle between every two adjacent segments is limited. We define

$$S_4 = \frac{TD_3 - \left| DP_1 - DP_2 \right|}{TD_3 \cdot A_3},$$

where TD_3 is the threshold of the direction difference, $\overrightarrow{DP_1}$ is the direction from the previous linked pixel to the current pixel, $\overrightarrow{DP_2}$ is the direction from the current pixel to the candidate pixel, and A_3 is a scalar for weighting.

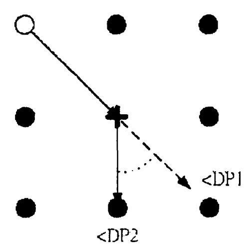

Fig. 5: Illustration of S_4

5) After score (1)–(4) has been calculated, the final measurement S is calculated as their product.

$$S = \prod_{i=1}^{4} S_i$$

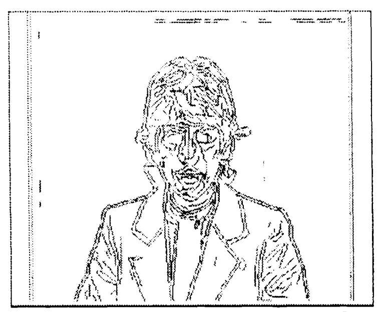
Fig. 6: Extraction of high curvature features

3.2.2 FEATURE LINKING

We wish the built mesh could retain the shape of objects. Hence, the high-curvature points around the object boundaries are extracted first. After the extraction of feature points, we link these feature points into curves and then use the linked curves as constraints for the following Constrained Delaunay Triangulation process. Our linking strategies are stated as follows:

1) Start at a pixel (p_1), whose curvature measurement is larger than a predefined threshold.
2) Search the eight-connection points of the pixel and use the similarity measures to decide whether the candidate pixels can be linked to the current pixel.

3) If the length of a linked line is shorter than the chosen threshold, ignore the line and start to link another line. If the length of the linked line is longer than the threshold, keep the line in the database.
4) Repeat Step 2 and Step 3 until no other features can be found.

3.3 SPLITTING METHOD

For an efficient representation, piecewise line segments can be used to approximate these linked curves. Then, we only need to record the endpoints of those line segments, instead of all the feature points on curves. We employ a splitting method described below to do curve approximation and Fig. 7 illustrates the splitting procedure.

1) Given a curve as shown in Fig. 7(a), draw a straight line between the two end-points.
2) Compute the distance between the original curve and the approximated curve. If the maximal distance is less than the threshold, stop.
3) Otherwise, add an additional point at the place where the maximal distance occurs. Replace the segment with two new segments. (Fig. 7(b), (c))
4) Recursively apply Step 2 and Step 3 to these new segments until the approximated curve is close enough to the original curve. (Fig. 7(d))

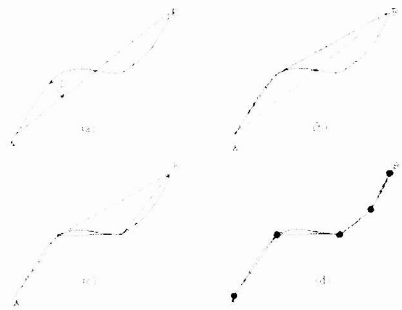

Fig. 7: The procedure of the splitting method

The end-points of these piecewise line segments are used as the representative points of the linked curves. We use these points and their interconnections to perform Constrained Delaunay Triangulation to generate the mesh for the original image.

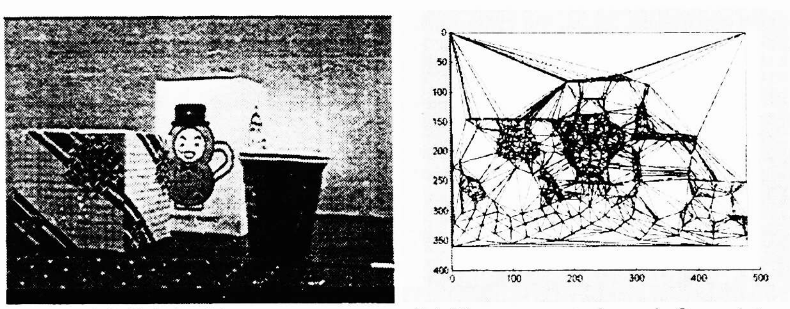

(a) Original image (b) The generated mesh from (a)

Fig. 8: The generation of a mesh object

4. HIERARCHICAL MESH OBJECT GENERATION

A hierarchical mesh structure may have two major advantages: 1) it can be transmitted progressively; 2) it can facilitate the tracking of mesh. There have been many algorithms to construct a hierarchical mesh based on a coarse-to-fine strategy. Node decimation and edge or triangle collapse are commonly used in currently available algorithms. Once a mesh is built, those methods generate a rough estimation of the mesh by removing unimportant nodes or by merging some similar patches. Since these procedures start from a finer resolution, the number of mesh nodes or patches is large at the first stage and the removal of nodes or the merging of patches is very expensive. Besides, the features are usually cluttered. Such a fine-to-coarse method is easy to implement but is time-consuming. Opposite to these approaches, our procedure is a coarse-to-fine scheme. We use a multi-resolution technique to build a three-layer pyramid. We generate a mesh for each layer and then eliminate duplicate mesh nodes to automatically form a hierarchical structure. In a fine-to-coarse strategy, all mesh nodes are tracked at the same time. After that, the motion vector of each node is transmitted accordingly based on which layer it belongs to. On the contrary, a coarse-to-fine strategy divides a complicated problem (tracking all mesh nodes) apart to reduce complexity. Mesh nodes on the coarser resolution layer are tracked first. These tracking results can help the tracking of mesh nodes on a finer layer. Because the movement on a coarser layer may offer a rough estimation, the motion vector on a finer layer can be found more efficiently.

In addition, a single-scale operator usually cannot extract all the features on various scales. In Fig. 8, it can be seen that the image is somehow over-segmented. To extract all the important features, a multi-resolution approach is employed to reduce computation complexity. Features appearing in coarser resolution are thought to be more important, and a multi-resolution approach has the inherent ability of importance classification. We can assign different degrees of importance on the generated nodes and edges. If the nodes are extracted from the lower resolution layer, they are treated as more important and are assigned a larger weight. This hierarchical mesh structure may facilitate the motion estimation of the mesh objects. The steps of hierarchical mesh generation is briefly described as below:

1) Construct a three-layer pyramid by down-sampling the original image twice.
2) Extract the feature points on all three layers.
3) For each layer, link the feature points into curves and use piecewise segments to approximate them.
4) Map the pixels on a linked curve to the corresponding pixels on the middle-resolution layer and mark these pixels with higher weights.
5) Link the feature pixels at the middle-resolution layer into piecewise line segments. If the number of the pixels that are marked higher weight (that means they may be mapped from the lower-resolution layer) predominates the pixel number of the line, mark this line with a higher weight. The lines that have no counterpart on the lower-resolution layer are marked with lower weights.
6) Repeat the above two steps on the highest-resolution layer. We classify the linked lines into three groups according to their weights. The lines with higher weights indicate they are extracted from the lower-resolution layers.

Based on the above procedure, we can generate the hierarchical mesh of an image. If we need the rough description of the image, we may only use the nodes and edges that are generated under the coarsest resolution. If we need a more detail view of the image, we use the nodes and edges generated in the higher-resolution layers. Fig. 9 shows the hierarchical mesh and the reconstructed intensity information.

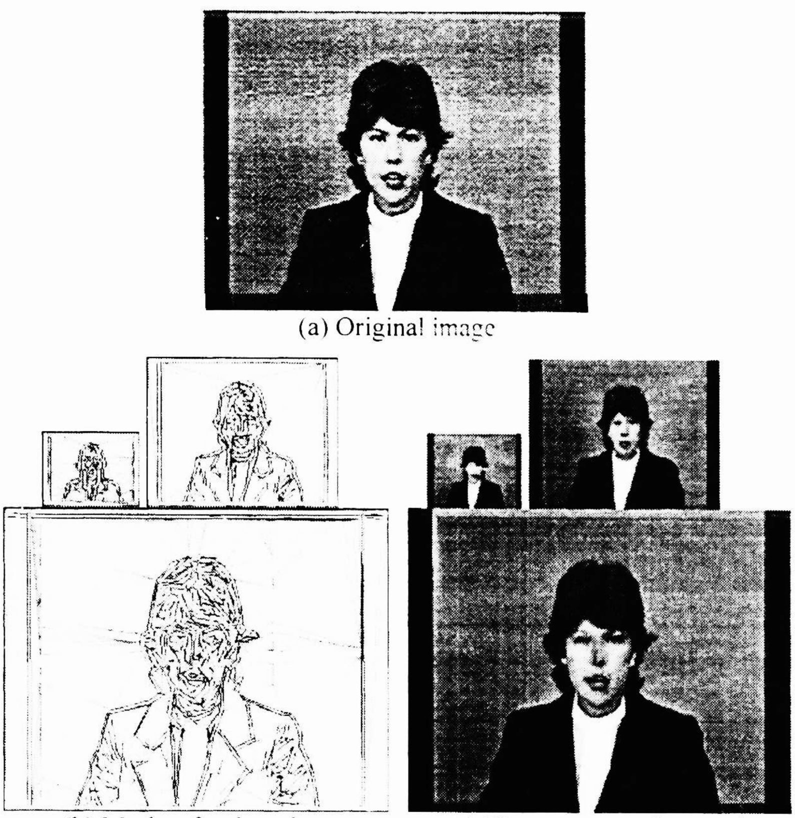

(a) Original image

(b) Meshes for three layers (c) The reconstruction results

Fig. 9: An example of a hierarchical mesh

5. TRACKING OF DYNAMIC MESH

So far, we have generated a hierarchical mesh to represent a still image. For an image sequence, it can be thought as deforming a mesh accordingly. We can record the trajectories of mesh nodes to represent those moving pictures. For this purpose, a primitive, nodal block matching method is used to track the mesh nodes. Depending on feature locality, feature strength, and intensity, we search the best matching mesh node in the next frame. We benefit from the hierarchical meshes of the image frames, as mentioned before, to facilitate node tracking. The tracking steps are shown as follows.

1) Initially, perform the node tracking on the lowest-resolution layer by using a nodal block-matching method.
2) While tracking the current mesh, there are two cases:
   A. on the previous coarser layer, if there is one node (eg., **a'**) that is mapped to the current node (eg., **a**), we can quickly and accurately track the current node **a** according to the motion of **a'**. In this example, we only need to search within Area A to find the best matching pixel for pixel **a**.
   B. Otherwise, the mesh node will be tracked directly by nodal block matching, like the point **b** in Fig. 10.
3) Repeat Step 2 until all the motion vector of the mesh nodes in the finest mesh have been found.

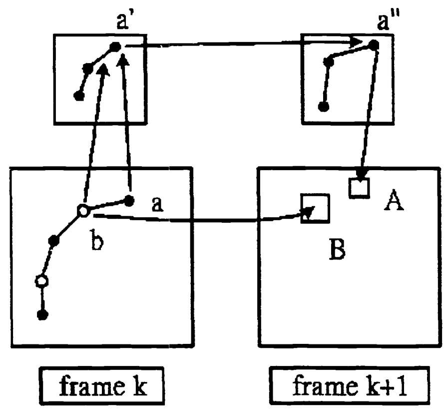

Fig. 10: A hierarchical matching of mesh nodes

In our experiments, we use the Claire sequence (288x360) as a test sequence. In Fig. 11, we show the tracking results of the first four frames. The left-hand side shows the original images (from top to bottom in increasing order) and the right-hand side shows the reconstructed images after tracking. Due to an inadequate number of mesh nodes and errors in the estimation of the motion vectors, the reconstructed images are a little distorted (see the face in Fig. 11). In practical, the quality of the reconstructed images can be improved by increasing the number of mesh nodes and some post-processing.

6. CONCLUSION

In this paper, we propose a different approach to generate hierarchical mesh objects. With this mesh structure, an image can be easily reconstructed back by simple linear interpolation. We also use a primitive method to track the generated mesh object in an image sequence. The simulation result shows that the usage of the high-curvature features simplifies the reconstruction process and the coarse-to-fine strategy may greatly reduce the complexity of motion tracking.

REFERENCE

1. L. Y. Wang and A. Vetro, "Use of two-dimensional deformable mesh structures for video coding, Part II — The analysis problem and a region-based coder employing an active mesh representation", *IEEE Trans. on Circuits and Systems for Video Technology*, vol. 6, no. 6, pp. 647-659, Dec. 1996.
2. Y. Wang and O. Lee, "Use of two-dimensional deformable mesh structures for video coding, Part I — The synthesis problem: Mesh-based function approximation and mapping", *IEEE Trans. on Circuits and Systems for Video Technology*, vol. 6, no. 6, pp. 636-646, Dec. 1996.
3. S.H. Jong, "The extraction of the high-curvature feature points in image surface", *M.S. thesis, National Chiao Tung University*, Hsinchu, Taiwan, ROC, 1998.

4. J. R. Shewchuk, "Triangle: Engineering a 2-D quality mesh generator and delaunay triangulator", *Applied Computational Geometry*, pp. 124-133, May 1996, Philadelphia, Pennsylvania, also available at http://www.cs.cmu.edu/quake/triangle.html.
5. James D. Foley, Andries van Dam, Steven K. Feiner, and John F. Hughes, Computer Graphics—Principles and Practice, 2nd in C, ADDISON-WESLEY.
6. K. Reinhard, "Mutiresolution representations for surfaces meshes based on the vertex decimation method", *Comput. & Graphics*, Vol. 22, No. 1, pp. 13-26, 1998.
7. Miguel Angel García, Angel Domingo Sappa and Luis Basañez, "Fast generation of adaptive quadrilateral meshes from range images", *Proceedings of the 1997 IEEE International Conference on Robotics and Automation Albuquerque*, New Mexico, April 1997.
8. Roberto Grosso, Christoph Lürig, and Thomas Ertl, "The multilevel finite element method for adaptive mesh optimization and visualization of volume Data", *Proceedings of Visualization '97*, pp. 387-394, 1997.
9. Mark Shackleton, " Learned deformable templates for object recognition", IEE Colloquium on Genetic Algorithms in Image Processing and Vision, pp. 7/1 – 7/6, 1994.
10. Concettina Guerra, "2D object recognition on a reconfigurable mesh", *Pattern Recognition*, Vol. 31, No. 1, pp. 83-88, 1998.
11. K. Hara, H. Zha, T. Hasegaa and T. Nagata, "3-D object modeling based on surface reconstruction and integration using optimal polygonal approximation", *IEEE International Conference on Computational Cybernetics and Simulation*, Vol. 3, pp.2644-2649, 1997.
12. Cheng-Yuan Liou and Quan-Ming Chang, "Meshed snakes", *IEEE International Conference on Neural Networks*, Vol. 3, pp. 1516-1521, 1996.
13. Candemir Toklu, A. Tanju Erdem, and A.M. Tekalp, "2-D mesh-based synthetic transfiguration of an object with occlusion", *IEEE International Conference on Acoustic, Speech, and Signal Processing*, Vol. 4, pp. 2649-2652, 1997.
14. Y. Wang and Jörn Ostermann, "Evaluation of mesh-based motion estimation in H.263-like coders", *IEEE Transactions on Circuits and Systems for Video Technology*, Vol. 8, No. 3, June 1998.
15. Peter van Beek, A.M. Tekalp, Ning Zhuang, Işil Celasun, and Minghui Xia, "Hierarchical 2-D mesh representation, tracking, and compression for object-based video", *IEEE Transactions on Circuits and Systems for Video Technology*, Vol. 9, No. 2, March 1999.
16. Yucel Altunbasak and A.M. Tekalp, "Occlusion-adaptive, content-based mesh design and forward tracking", *IEEE Transactions on Image Processing*, Vol. 6, No. 9, September 1997.

Left: The Original Sequence Right: The Experiment Result

Fig. 11: The tracking result for the first 4 frames of the Claire sequence